

V. A. Fal'kovskii, M. V. Kuralina,  
G. G. Travushkin, and Yu. E. Tyablikov

UDC 620.153.2:669.275

The selection of the grade of the hard alloy ensuring the highest efficiency of the instrument is associated with the analysis of the mechanical properties determined in laboratory conditions and depends on the results of long-term tests in production conditions.

The mechanical properties of the hard alloys, such as the ultimate strength in bending and compression, yield stress, limiting residual strain, and specific work of fracture, determined in static loading of specimens of the hard alloy, do not simulate the conditions of the stress state formed in service. In production conditions, it is usually necessary to test several grades of hard alloys and this is very expensive.

Loading of the hard alloys is accompanied by the formation of defects in the alloy which influence the mechanical properties and efficiency of the hard alloy [1]. Therefore, in selecting the most efficient hard alloy for a specific type of instrument, it is necessary to develop a test method which would make it possible to reproduce, in the laboratory conditions, the most important (main) service parameter which determines the efficiency of the alloy.

In this work, we present the results of examination of contact fatigue with continuous recording of damage in compression loading of hard alloys to be used for cutting dies.

Investigations were conducted into the properties of new alloys produced on the basis of high-temperature powders, i.e., coarse-grain powders with a tungsten-carbide grain size of 3.5-4  $\mu\text{m}$  (VK10KS, VK15KS, and VK20KS) and medium-grain powder with a grain size of 2.2-2.5  $\mu\text{m}$  (VK15S). For the sake of comparison, VK20 standard alloy with a grain size of 2.2-2.5  $\mu\text{m}$  which is used most extensively at the present time for cutting dies was tested. This alloy is produced on the basis of low-temperature powders of W and WC.

Figure 1 shows the diagram of the properties and efficiency (EF) of the examined alloys and grades. The deformation characteristics of the alloys, including the yield stress, the limiting residual strain, and the specific work of plastic deformation, were determined in stepped loading (with 0.1-0.4 MPa steps) of rectangular specimens (7 x 7 x 14 mm) in uniaxial compression. The yield stress determined from the stress-strain curve in the semi-logarithmic coordinates corresponded to the stress at a residual strain of 0.1%. The limiting value of residual strain prior to fracture was determined by extrapolating the stress-strain curve to the fracture stress. The value of the specific work of deformation, determined graphically, is equal to the area delineated by the strain curve, the ordinate of the fracture load, and the abscissa (strain axis).

Efficiency was determined as the mean durability between regrinding the dies up to a specific criterion of blunting in the operation of cutting out grooves in rotor blades 0.5 mm thick made of a transformer steel. The blunting criterion was represented by the size of the burr on the cut blades of 0.05 mm. The dies were tested at the Scientific-Research Institute of the Tallin Electrotechnical Plant. Blanks of simple form for punches and matrices of the cutting dies were produced from the selected alloys in the laboratory conditions of the All-Union Scientific-Research and Design Institute of Refractory Metals and Hard Alloys. The electrospark treatment of the blanks and their diamond polishing and finishing treatment were carried out at the Scientific-Research Institute of the Tallin Electrotechnical Plant. Experimental stamps to be tested in semiautomatic equipment manufactured by Schuler Company (West Germany) were also produced at this institute.

The test results show that the highest durability between regrinding is exhibited by VK15S alloy ( $\sim 990,000$  stamping strokes) characterized by the optimum combination of the

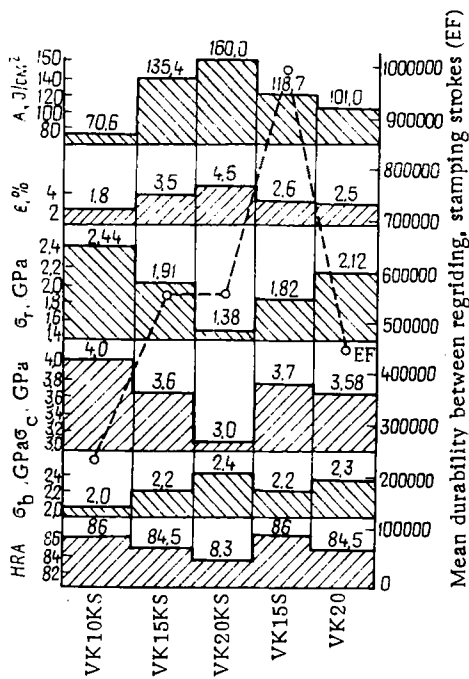


Fig. 1. Mechanical properties (hardness HRA, ultimate strength in bending  $\sigma_b$  and compression  $\sigma_c$ , yield stress  $\sigma_{T0.1}$ , the limiting value of residual strain prior to fracture  $\epsilon$ , specific work of plastic deformation prior to fracture A) and efficiency EF (the number of stamping strokes between regrinding) of the examined grades of the WC-Co hard alloys.

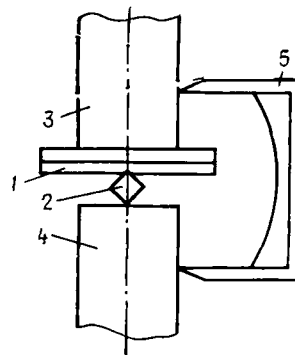


Fig. 2. Diagram of loading of the specimens in examining contact fatigue in compression: 1, 2) tested specimens; 3, 4) supports; 5) strain gage.

properties for the given application conditions (high ductility and strength properties combined with increased hardness).

At the same time, as indicated by Fig. 1, this alloy does not have the maximum strength and ductility properties which could be considered in selecting the alloy ensuring the highest efficiency of the instrument in service.

In addition to this, it should be mentioned that the mechanical properties are determined in the conditions of static loading whereas in service the alloy is subjected to cyclic loading.

Low-cycle fatigue was examined on rectangular specimens ( $5 \times 5 \times 20$  mm). Bevels 0.5 mm wide were ground at an angle of  $45^\circ$  at the edges of the specimens. The length of the specimen (20 mm) was selected such as to avoid interfering with installation of strain gages for recording the extent of mutual penetration of the specimens in the individual cycles. The specimens were placed on special supports whose edges were machined to the form corresponding to the profile of the specimen (round or rectangular - Fig. 2). Prior to this operation, the special supports were fixed in clamps on a UME-10TM testing machine. The supports were made of an alloy whose modulus of elasticity and hardness were higher than those of the examined alloys. Since the strain in the supports in reference experiments was insignificant in comparison with the value  $\Delta \epsilon_i$ , the strain in the supports can be ignored.

TABLE 1. Damage Cummulation in Low-Cycle Fatigue

| Cycle No. | Value of 'quasiplastic' strain $\Delta l_i$ , $\mu\text{m}$ , for alloys |                                 |                                 |                                 |      |
|-----------|--|---------------------------------|---------------------------------|---------------------------------|------|
|           | VK10-KS  | VK15-KS                         | VK20-KS                         | VK15-S                          | VK20 |
| 2         | 6  | 7                               | 12                              | 1                               | 9    |
| 3         | 11   | 12                              | 22                              | 1,75                            | 16   |
| 4         | 14   | 16                              | 29                              | 2,50                            | 21   |
| 5         | 16   | 19                              | 34                              | 3,0                             | 24   |
| 6         | 18   | 21                              | 38                              | Start of the steady-state stage | 27   |
| 7         | Start of the steady-state stage  | 23                              | 41                              |                                 | —    |
| 8         |  | Start of the steady-state stage | 43                              | —                               |      |
| 9         | —  |                                 | —                               |                                 | —    |
| 10        | —  | —                               | Start of the steady-state stage | —                               |      |

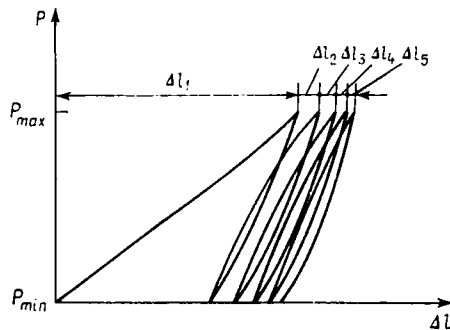


Fig. 3. Diagram of cyclic loading specimens of hard alloys ( $\delta l_1 \gg \Delta l_2 > \Delta l_3 > \Delta l_4 > \Delta l_5$ ).

After positioning the specimen, a specific initial load (lower than load  $P_{min}$  in cyclic loading) was applied to the specimen. In loading with  $P_{min}$  a strain gage was placed on the special supports and used to record the depth of mutual penetration of the examined specimens determined by the degree of damage in the materials and by the magnitude of the plastic strains in the specimens. In this method, the scale for recording the depth was selected from the following values:  $2000 \times 1$ ;  $1000 \times 1$ ;  $800 \times 1$ ;  $600 \times 1$ ;  $400 \times 1$ ;  $200 \times 1$ .

The fatigue loading parameters were continuously recorded during testing.

In cyclic loading, the specimens penetrate into each other as a result of plastic deformation and of microfailures on the contacting surfaces. This penetration which we shall refer to as 'quasiplastic' deformation was recorded by UME-10TM diagram-drawing device in the load-quasiplastic strain coordinates (Fig. 3). In analysis of this diagram, we constructed the dependences of the variation of the parameter of damage cumulation  $\Delta l_i$  with respect to the individual cycles.

The specimens of the examined alloys were loaded in the conditions  $P_{min} = 0.0005 \text{ MN}$ ,  $P_{max} = 0.004 \text{ MN}$ , with a loading frequency of 3 cycles/min. The test results are presented in Table 1.

As indicated by the data in Table 1, the magnitude of the quasiplastic strain in cyclic loading greatly differs for the examined alloys. For example, VK15-S alloy showed considerably lower values of  $\Delta l_{1-5}$  in the first loading cycles.

For the specimens of all the alloys, the load-quasiplastic strain curve after 10-15 cycles showed a horizontal section indicating the start of the stage of steady-state damage. The increment of quasiplastic strain  $\Delta l$  in this stage in calculations per cycle in the cycle range from 20 to 500 cycles for the VK15-S alloy is equal to  $0.2 \mu\text{m}$ , for VK10-KS alloy it is  $0.28 \mu\text{m}$ , for VK15-KS  $0.37 \mu\text{m}$ , for VK20-KS  $0.67 \mu\text{m}$ , and VK20  $1.5 \mu\text{m}$ . For the given alloy, the value of  $\Delta l$  is constant in the selected loading conditions.

In the range of 20-500 load cycles, some of the alloys showed a jump-like change of  $\Delta l$  in the hardening stage; this change indicates that single damage acts take place. This nature of the state of damage causes VK20 alloy to differ from other examined alloys.

Computing the values of  $\Delta l_{fr}$  and  $\Delta l_{plast.def.}$  from the diagram, we can determine the relationship between microfracture and microplastic deformation. For the alloys made on the basis of the low-temperature powders of tungsten and tungsten carbide (VK20), the value of microfracture is comparable with the value of microductility, whereas for the alloys produced using the high-temperature powders, the microfracture value is an order of magnitude lower than the value of microplastic strain.

In subsequent cyclic loading, both in the laboratory conditions and in stamping the steel in service of the dies, microfractures cumulate and localize in a specific volume. The reduced resistance to microfracture detected in low-cycle fatigue determines the reduction of the endurance of material in service.

Thus, the value of quasiplastic strain  $\Delta l_{const}$  characterizes the resistance of the material to damage (in the given conditions of cyclic compression loading). The reduction of  $\Delta l_{const}$  and of the rate of increase of  $\Delta l_i$  to the steady-state stage (to the hardening stage) increases the resistance of the material to microfracture and microplastic deformation. Consequently, the parameters indicating the behavior of the material in the stages of damage cumulation and hardening in the conditions of low-cycle fatigue in compressive loading are new characteristics which make it possible to evaluate more accurately the behavior of the hard alloy in service.

On the basis of the data presented in Table 1 it may be concluded that VK15-S alloy is the most suitable alloy for components working in the conditions of fatigue contact loading. This alloy is characterized by considerably higher resistance to damage in fatigue contact loading both in the initial (up to 10 cycles) and the steady-state stage, and is characterized by the highest efficiency in the die in cutting grooves in the blades of the rotor of the electric motor (Fig. 1).

#### CONCLUSIONS

1. The proposed experimental method of examining the resistance to low-cycle fatigue makes it possible to approximate the laboratory conditions to the real loading conditions and predict the behavior of the alloy in service [2].
2. The alloys produced from the high-temperature powders of tungsten and tungsten carbide have higher resistance to microfracture in comparison with the alloys based on the low-temperature powders (VK20).
3. The highest parameters of the resistance of damage and efficiency in stamping were recorded for VK15-S alloy.

The authors are grateful to their colleagues V. I. Tumanov and V. F. Ochkasov for the determination of the mechanical properties of the hard alloys using the procedures in accordance with GOST, and to Kh. D. Reshetnyak and G. P. Viktorov for organizing the tests of the alloys in the production conditions.

#### LITERATURE CITED

1. V. A. Ivensen, V. A. Fal'kovskii, I. V. Chumak, and T. N. Proshkina, "Changes of the mechanical properties of a hard alloy in plastic deformation," *Izv. Akad. Nauk SSSR, Met.*, No. 2, 140-144 (1975).
2. V. A. Fal'kovskii, M. V. Kuralina, et al., "A method of testing the contact strength of material," *Inventor's Certificate No. 939995, Byull. Izobret.*, No. 24 (1982).